Journal of Solid State Chemistry 181 (2008) 1723–1730

Contents lists available at ScienceDirect

Journal of Solid State Chemistry

journal homepage: www.elsevier.com/locate/jssc

# Syntheses and characterization of elpasolite-type ammonium alkali metal hexafluorometallates(III)

Jin-Xiao Mi [a,b,*], Shu-Ming Luo [a], Hua-Yu Sun [a], Xiao-Xuan Liu [a], Zan-bin Wei [c]

[a] Department of Materials Science and Engineering, College of Materials, Xiamen University, Xiamen 361005, PR China
[b] Key Laboratory of New Processing Technology for Nonferrous Metals and Materials (Ministry of Education), Guilin University of Technology, Guilin 541004, PR China
[c] Department of Chemistry, College of Chemistry and Chemical Engineering, Xiamen University, Xiamen 361005, PR China

ARTICLE INFO

*Article history:*
Received 31 October 2007
Received in revised form
17 March 2008
Accepted 22 March 2008
Available online 27 March 2008

*Keywords:*
Elpasolite
Hydrothermal synthesis
Crystal structure
Effective ionic radius
Ammonium ion

ABSTRACT

Crystal structures of three fluorides $(NH_4)_2NaFeF_6$, (**Fe**), $(NH_4)_2NaGaF_6$, (**Ga**), and $(NH_4)_2NaCrF_6$, (**Cr**), as well as a substituted compound $[(NH_4)_{1-x}K_x]_2KAlF_6$ ($x \approx 0.17$), (**Al**), have been refined using single-crystal and powder X-ray diffraction techniques. All these four ammonium hexafluorides have a cubic elpasolite-type structure and crystallize in the space group $Fm\bar{3}m$ with lattice constants $a = 8.483(3)$, 8.450 (3), 8.4472(2) and 8.724(3) Å for compounds (**Fe**), (**Ga**), (**Cr**) and (**Al**), respectively. The effective ionic radius of the ammonium ion calculated from those compounds has a mean value of $R = 1.729$ Å for CN = 12. An ultraviolet–visible absorption spectrum of $(NH_4)_2NaCrF_6$, measured at room temperature, gives a crystal field ($Dq = 1575\,cm^{-1}$) and Racah parameters ($B = 758\,cm^{-1}$ and $C = 3374\,cm^{-1}$). Abnormal anisotropic thermal parameters of fluorine atoms have been observed in the compound (**Al**), and interpreted to arise from four strong hydrogen bonds (F…H–N) that are distributed in a square form around each fluorine atom.



## 1. Introduction

There is a large family of $A^I_2B^IM^{III}F_6$ compounds ($A^I$, $B^I$ monovalent cations; $M^{III}$ trivalent cation) with an elpasolite ($K_2NaAlF_6$) or cryolite ($Na_2NaAlF_6$, when $A = B$) structure derived from a perovskite superstructure with doubled cell edges [1,2]. In this family, the compounds generally crystallize in the face-centered cubic system at room or high temperatures, but are commonly trigonal, tetragonal or even monoclinic, especially after structural phase transitions, at low temperature. The cubic compounds with the highest symmetry (i.e. $Fm\bar{3}m$) are well suited for testing the validity of Pauling's rules, calculating the radii of ions, and evaluating the bond-valence parameters. Ever lasting, considerable interest has been focused on the structural studies at different pressures/temperatures of transition metal fluorides, particularly those containing Jahn–Teller distortions and phase transitions via order–disorder transformation [3–5]. Also, there is much current interest in $Cr^{3+}$-doped fluoride crystals for potential application as tunable solid-state lasers operating at room temperature [6–9].

Although there is a considerable literature on the synthesis of various ammonium hexafluorometallates(III), only a few studies investigated their crystal structures. The reported compounds of the cryolite-type structure include $(NH_4)_3M^{III}F_6$($M^{III}$ = Al, Sc, V, Cr, Fe, Ga, In) [10–12], while those of the elpasolite-type structure are $(NH_4)_2NaM^{III}F_6$ ($M^{III}$ = Al, Fe, Ga, In, Cr, V) [13–15], $(NH_4)_2KM^{III}F_6$ ($M^{III}$ = Fe, Ga, Cr, V), $Cs_2(NH_4)M^{III}F_6$ ($M^{III}$ = Al, Fe, Ga, Cr, V) [16] and $[(NH_4)_{2-x}K_x]KAlF_6$( $0 \leqslant x \leqslant 1$) [17]. For these ammonium hexafluorometallates, different methods have been developed for their syntheses. The most popular ones involve various solid-state reactions such as the one used in the preparation of $Cs_2(NH_4)GaF_6$, which was synthesized at 700 °C in a platinum tube sealed under an inert atmosphere [5]. Also, the solution route has been used (e.g., $(NH_4)_3FeF_6$ [10]). In addition, a hydrothermal method has been used for both $(NH_4)_2NaInF_6$ [14] and $(NH_4)_2NaAlF_6$, and the crystal structure for the latter was refined by our group recently [15]. This hydrothermal method has opened a fruitful route for the synthesis of new compounds that are difficult or impossible to obtain by high-temperature solid-state reactions. Herein we report on the synthesis of four ammonium fluoride compounds by use of a simple hydrothermal method.

Of all four cubic ammonium fluorides $(NH_4)_2NaFeF_6$, $(NH_4)_2NaGaF_6$, $(NH_4)_2NaCrF_6$ and $[(NH_4)_{1-x}K_x]_2KAlF_6$ ($x \approx 0.17$) reported herein, complete structures such as atomic coordinates have not been reported. For example, little structural information is available about $(NH_4)_2NaCrF_6$, except its synthesis, chemical composition and cell parameters [13]. Herein we present a detailed characterization of the four cubic ammonium fluorides by use of SEM, IR and UV–vis and single-crystal and powder X-ray structural analysis.

* Corresponding author at: Department of Materials Science and Engineering, Xiamen University, Siming Southern Road, No. 422, Xiamen, Fujian Provience 361005, PR China. Fax: +86 592 2183937.
*E-mail address:* jxmi@xmu.edu.cn (J.-X. Mi).

0022-4596/$ - see front matter © 2008 Elsevier Inc. All rights reserved.
doi:10.1016/j.jssc.2008.03.017

## 2. Experimental

### 2.1. Syntheses

All compounds reported here were synthesized by using hydrothermal method. For example, a mixture of $NaHF_2$ (51 mg), $NH_4H_2PO_4$ (1024 mg), $CrCl_3$ (50 mg), HCl (0.6 ml, 37%) and 9 ml of distilled water with a molar ratio $NH_4$:Na:Cr:F = 33:2:1:27 was used for the synthesis of $(NH_4)_2NaCrF_6$, (**Cr**). All starting materials were of analytical grade purity and used as received without further purification. The above mixture was sealed into a 30-mL Teflon-lined stainless steel autoclave, heated at 453 K for 5 days and then cooled to room temperature at a rate of 10 K/h. The resulting cyan-green powder was filtered off, washed with distilled water, and then dried in a desiccator at ambient temperature. The polycrystalline powder was confirmed as a single phase and identified as the compound (**Cr**) by X-ray powder diffraction analysis.

Similarly, both $(NH_4)_2NaFeF_6$, **(Fe)** and $(NH_4)_2NaGaF_6$, **(Ga)** were prepared by use of this procedure, except that Fe (50 mg) and Ga (45 mg) metals, respectively, instead of $CrCl_3$ were used. In the Fe-bearing runs, sporadic colorless, octahedral faceted crystals of the compound **(Fe)** were obtained and wrapped in a polycrystalline white powder. Powder X-ray diffraction analysis revealed at least three phases, including $Fe(NH_4)HP_3O_{10}$. In order to obtain a pure product, various attempts including (1) using $(NH_4)Cl$ instead of $NH_4H_2PO_4$, (2) changing the molar ratios of the reactants, (3) different reaction temperatures, and (4) different degrees of filling and pH values have been made but were not successful. Our study showed that $NH_4H_2PO_4$ plays a critical role in the syntheses of the compound **(Fe)** in this route. A similar situation has been observed in the preparation of the compound **(Ga)**, which is also octahedral in shape and wrapped in a white powder of $Ga(NH_4)HP_3O_{10}$. The compound $[(NH_4)_{1-x}K_x]_2KAlF_6$ ($x \approx 0.17$), **(Al)** was obtained by use of a mixture of KOH (136 mg), $H_3BO_3$ (150 mg), $NH_4F$ (300 mg), $AlCl_3 \cdot 6H_2O$ (153 mg) and 10 ml of distilled water with a molar ratio K:$NH_4$:Al :F = 2.4:8:1:8.

The presences of Ga, Fe, Cr, Na, K and F in the products have been confirmed by semi-quantitative chemical analysis carried out on an Oxford Instruments Energy Dispersive Spectrometer (EDS). Also, phosphorus and chlorine have been detected in all four compounds. The contents of nitrogen and hydrogen in the compound (**Cr**), determined on an EA-MA1110 elemental analyzer (Carlo Erba, Milan, Italy), were found to be 12.56 wt% (vs cal. 12.45 wt%), 3.49 wt% (vs cal. 3.58 wt%), respectively.

### 2.2. Spectroscopy

Fourier transform infrared (FTIR) spectra in the range of 4000–370 $cm^{-1}$ have been obtained by use of 2 mg samples dispersed in 200 mg KBr and a Nicolet Avatar 360 FTIR spectrometer (resolution $<2\ cm^{-1}$). The FTIR spectrum of the compound **(Cr)** is illustrated in Fig. 1, whereas those of compounds **(Ga)**, **(Fe)**, and **(Al)** are not present here and are more complicate owing to the presence of other phases. A Raman spectrum of the compound **(Cr)** in the frequency range of 3500–150 $cm^{-1}$ (Fig. 2) was measured on a Renishaw UV–vis Raman System 1000 spectrometer, using an argon laser excitation at 514.5 nm (resolution $<2\ cm^{-1}$). An ultraviolet–visible absorption spectrum of the compound **(Cr)** (Fig. 3) was recorded at room temperature on a Shimadzu UV-2501 PC spectrophotometer with slits set to 1 nm.

### 2.3. Crystal structural determination

The crystal structures of the as-prepared compounds of **(Fe)**, **(Ga)**, and **(Al)** have been investigated on selected single crystals using a Bruker Smart CCD detector (Mo$K\alpha$ radiation, graphite monochromator, 50 kV/40 mA, scan types $\phi$ and $\omega$) at 295 K. The X-ray raw data were corrected for Lorentz and polarization effects. An empirical absorption correction was also applied. The structures were solved by direct methods and refined by the

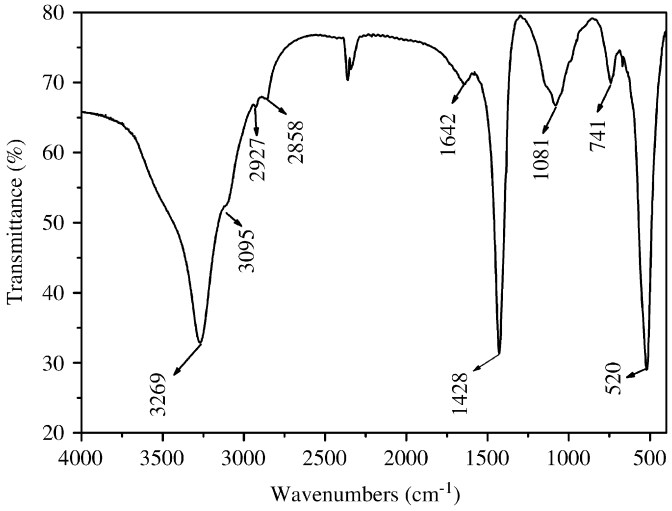


**Fig. 1.** FTIR spectrum of $(NH_4)_2NaCrF_6$.

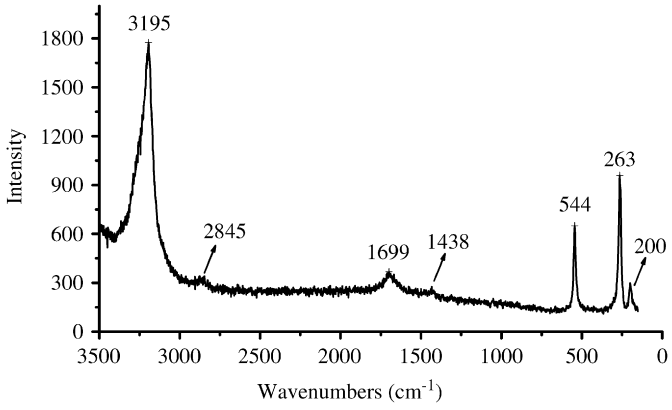


**Fig. 2.** Raman spectrum of $(NH_4)_2NaCrF_6$.

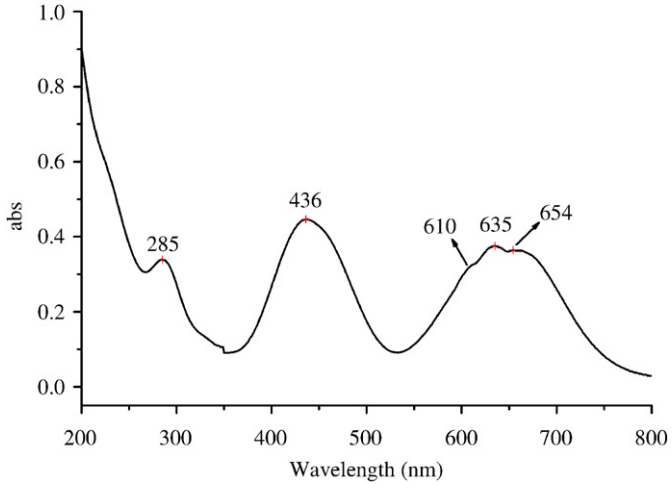


**Fig. 3.** Ultraviolet–visible absorption spectrum of $(NH_4)_2NaCrF_6$.

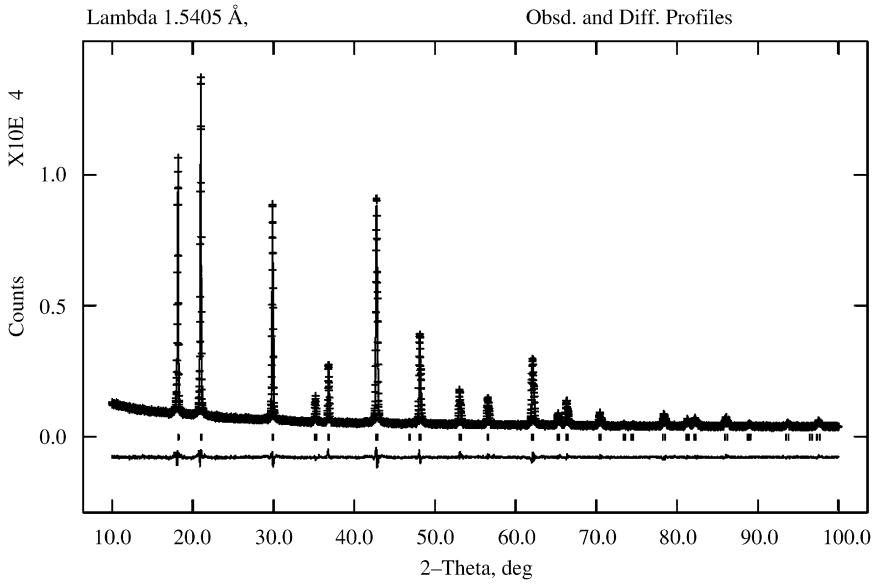


**Fig. 4.** A comparison of observed (top crosses) and calculated (top solid line) intensity profiles for $(NH_4)_2NaCrF_6$; intensity differences (bottom solid line) and allowed Bragg reflections (tick marks) are also shown.

full-matrix least-squares method using the SHELXS-97 and SHELXL-97 software packages [19]. After anisotropic refinement of the heavier atoms, hydrogen atom was located from the difference Fourier map and then refined by fixing its isotropic parameter and N–H distance (0.89 Å). Our structural refinement of the compound **(Al)** showed that the ammonium ion was partially substituted by potassium, which has a significantly larger X-ray scattering power than nitrogen.

The X-ray powder diffraction pattern of the compound **(Cr)** was collected on a Phillips Panalytical X-pert diffractometer using Cu$K\alpha$ radiation, monochromatized by a secondary graphite monochromator. The data were collected in the range between 10° and 100° $2\theta$ in steps of 0.008°. The atomic positions of the compound **(Fe)** were used as a starting model for Rietveld refinements using the GSAS program package [20]. Initially, scale, background, zero point and lattice parameters were refined. The structure was refined using the Rietveld method with isotropic displacement parameters, except fixing the hydrogen position and isotropic displacement from a starting model. The profile fitting of the final refinement was shown in Fig. 4.

The crystallographic data and refinement results, atomic coordinates and equivalent displacement, anisotropic displacement parameters, as well as selected interatomic distances and angles of the reporting compounds are summarized in Tables 1–4. Further details of the crystal structure investigation are available from the Fachinformationszentrum Karlsruhe, D-76344 Eggenstein-Leopoldshafen (Germany), on quoting the depository numbers CSD-418735, 418736, 418737, and 418738 for compounds **(Cr)**, **(Fe)**, **(Ga)**, and **(Al)**, respectively, the name of the authors, and citation of the paper.

## 3. Results and discussion

### 3.1. Structural description

All four ammonium hexafluorometallates(III) reported herein with a general formula of $(NH_4)_2B^{I}M^{III}F_6$ are isomorphic. In their structure as illustrated in Fig. 5, trivalent cations ($M$: $Al^{3+}$, $Ga^{3+}$, $Fe^{3+}$ or $Cr^{3+}$) occupy the corner (0, 0, 0) and face-center ($\frac{1}{2}$, $\frac{1}{2}$, 0) of the cube. Fluorine atoms are placed on the four-fold axis of the crystal to form a regular octahedron around each trivalent cation. Alkali cations (B: $Na^+$ or $K^+$) are located on the edge ($\frac{1}{2}$, 0, 0) of the cube, while nitrogen atoms are positioned in the tetrahedral sites ($\frac{1}{4}$, $\frac{1}{4}$, $\frac{1}{4}$), and are coordinated to four H atoms. [$BF_6$] and [$M^{III}F_6$] octahedra alternate along the three four-fold axes and are linked to each other by common F atoms located at the octahedral vertices. Cations B and M are located in the 4*b* and 4*a* sites of the $Fm\bar{3}m$ space group, respectively, whereas cation A occupies the 8*c* site with CN = 12. This type of structure, namely elpasolite ($A^{I}_2B^{I}M^{III}F_6$), is a perovskite superstructure with a doubled cell edge. It results from the substitution of two $M^{II}$ cations in $A^{I}_2M^{II}M^{II}F_6$ by two different ions $B^{I}$+$M^{III}$, which are ordered at the octahedral sites owing to differences in both charge and size [1], in $A^{I}_2B^{I}M^{III}F_6$.

In the structure of elpasolite ($K_2NaAlF_6$), much attention has been paid to the relationship between entropy change and order–disorder at phase transitions. It is well known that there is a large entropy change in ammonium cryolite, which has been explained by a model involving orientational disorder of both the ammonium and hexafluorometallate(III) ions. Structural refinement by Udovenko et al. [18] showed that fluorine atoms have abnormal large isotropic thermal parameters of 0.151(9) Å$^2$ and 0.076(8) Å$^2$ in the $(NH_4)_3FeF_6$ and $(NH_4)_3AlF_6$, respectively, if they are located at site 24*e*. Consequently fluorine atoms were believed to be in disorder in these two structures. In comparison, the compounds **(Ga)**, **(Fe)** and **(Cr)** have normal thermal parameters for all the atoms. However, in the compound $[(NH_4)_{1-x}K_x]_2KAlF_6$ ($x \approx 0.17$), **(Al)** exhibit abnormal anisotropic thermal parameters. For example, the values of $U_{11}$ (0.0897(14) Å$^2$) and $U_{22}$ (0.0897(14) Å$^2$) are much larger than that of $U_{33}$ (0.0142(12) Å$^2$). These data suggest that fluorine atoms in the compound **(Al)** are also distributed in a disorder mode, pointing to a possible phase transition at low temperature. The short $U_{33}$ axis coincides with the bond direction between potassium and fluorine, and the long $U_{11}$ and $U_{22}$ axes are associated with the hydrogen bonds of F···H–N, where each fluorine atom is surrounded by four hydrogen atoms in a square form as shown in Fig. 6. These results support data from a previous study on the endmember phases $[(NH_4)_{2-x}K_x]KAlF_6$($x = 0,1$), for which phase transitions occur at 250 and 186 K for the $x = 0$ composition and at 170 K for the $x = 1$ composition, respectively [17]. We believe that the

**Table 1**
Crystal data and structure refinements of $(NH_4)_2NaMF_6$ ($M$ = Ga, Fe, Cr) and $[(NH_4)_{0.83}K_{0.17}]_2KAlF_6$

| Formula | $(NH_4)_2NaGaF_6$ | $(NH_4)_2NaFeF_6$ | $[(NH_4)_{0.83}K_{0.17}]_2KAlF_6$ | $(NH_4)_2NaCrF_6$ |
|---|---|---|---|---|
| Formula mass (g/mol) | 242.79 | 228.92 | 223.32 | 225.05 |
| Space group, $Z$ | $Fm$–3$m$, 4 | $Fm$–3$m$, 4 | $Fm$–3$m$, 4 | $Fm$-3$m$, 4 |
| $a$ (Å) | 8.450(3) | 8.483(3) | 8.724(3) | 8.4472(2) |
| $V$ (Å$^3$) | 603.4(4) | 610.4(4) | 664.0(4) | 602.75(1) |
| Density (calc.) (g/cm$^3$) | 2.673 | 2.491 | 2.234 | 2.480 |
| Diffraction techniques | Single crystal | Single crystal | Single crystal | Powder diffraction |
| Temperature (K) | 293(2) | 293(2) | 293(2) | 293(2) |
| Radiation | Mo$K\alpha$, graphite | Mo$K\alpha$, graphite | Mo$K\alpha$, graphite | Cu$K\alpha$, graphite |
| Crystal size (mm$^3$) | Octahedron, colorless transparent, $0.05 \times 0.05 \times 0.06$ | Octahedron, colorless transparent, $0.08 \times 0.08 \times 0.10$ | Octahedron, colorless transparent, $0.11 \times 0.12 \times 0.17$ | Cyan-green opaque powder |
| $\mu$ (mm$^{-1}$) | 4.687 | 2.594 | 1.194 | |
| $2\theta_{max}$ (deg) | 55.60 | 55.36 | 55.80 | 100 |
| Miller-index range | $-10 \leqslant h \leqslant 11$, $-10 \leqslant k \leqslant 11$, $-10 \leqslant l \leqslant 10$ | $-9 \leqslant h \leqslant 10$, $-8 \leqslant k \leqslant 11$, $-11 \leqslant l \leqslant 11$ | $-8 \leqslant h \leqslant 11$, $-9 \leqslant k \leqslant 11$, $-10 \leqslant l \leqslant 9$ | $1 \leqslant h \leqslant 8$, $0 \leqslant k \leqslant 6$, $0 \leqslant l \leqslant 4$ |
| Total data collected | 1251 | 897 | 969 | |
| Unique data/ $I > 2\sigma(I)$ | 57, 57 | 58, 58 | 60, 62 | 58 |
| No. of parameters refined | 10 | 8 | 11 | 38 |
| $F(000)$ | 472 | 452 | 443 | 444 |
| $T_{min}$, $T_{max}$ | 0.7663, 0.7994 | 0.7814, 0.8193 | 0.8228, 0.8799 | |
| $R$, $R_w$(all data) | 0.0176, 0.0633 | 0.0216, 0.0749[a] | 0.0236, 0.0617 | 0.0346, 0.0446 |
| GOF | 1.571 | 1.418 | 1.194 | 1.16 |
| Largest diff. peak/hole (e/Å$^3$) | 0.276, −0.373 | 0.337, −0.656 | 0.224, −0.348 | |
| Software | SHEXL-97, SHEXS-97 | SHEXL-97, SHEXS-97 | SHEXL-97, SHEXS-97 | GSAS |

[a] Refinement on Fe atoms split into two positions in disorder mode gave occupancies in site ($\frac{1}{2}$, $\frac{1}{2}$, 0) with 96.3(8)% and in site ($\frac{1}{2}$, $\frac{1}{2}$, 0.207) with 3.7(8) % , and led to $R = 0.0163$ and $R_w = 0.0415$, as well as max diff. density 0.218 and min −0.230 e/Å$^3$.

**Table 2**
Atomic coordinates and isotropic displacement parameters (Å$^2$) for $(NH_4)_2NaMF_6$ ($M$ = Ga, Fe, Cr) and $[(NH_4)_{0.83}K_{0.17}]_2KAlF_6$

| Formulas | Atoms | Site | $x$ | $y$ | $z$ | $U_{iso}$ |
|---|---|---|---|---|---|---|
| $(NH_4)_2NaGaF_6$ | F1 | 24$e$ | 0.5000 | 0.5000 | 0.2242(4) | 0.0255(10) |
| | H1 | 32$f$ | 0.1903 | 0.3097 | 0.3097 | 0.080 |
| $(NH_4)_2NaFeF_6$ | F1 | 24$e$ | 0.5000 | 0.5000 | 0.2274(4) | 0.0289(9) |
| | H1 | 32$f$ | 0.1909 | 0.3091 | 0.3091 | 0.08 |
| $[(NH_4)_{0.83}K_{0.17}]_2KAlF_6$ | F1 | 24$e$ | 0.5000 | 0.5000 | 0.2050(3) | 0.0645(10) |
| | H1 | 32$f$ | 0.1910 | 0.3090 | 0.3090 | 0.072 |
| $(NH_4)_2NaCrF_6$ | F1 | 24$e$ | 0.5 | 0.5 | 0.22746(13) | 0.0315(12) |
| | H1 | 32$f$ | 0.1909 | 0.3091 | 0.3091 | 0.08 |

Trivalent cations (Al, Ga, Fe, Cr) locate at (0,0,0)(4a); while sodium or potassium cations at ($\frac{1}{2}$, $\frac{1}{2}$, $\frac{1}{2}$) (4b) and ammonium ions at ($\frac{1}{4}$, $\frac{1}{4}$, $\frac{1}{4}$) (8c). The effect of ammonium ions substituted with potassium cations about 17% in disorder was observed, resulting in a formula of $[(NH_4)_{0.83}K_{0.17}]_2KAlF_6$. $(NH_4)_2NaCrF_6$ was refined from powder technique with $U_{iso} = 0.0237(12)$, 0.0367(13), and 0.0279(15) for Cr, Na, and N atoms, respectively.

**Table 3**
Anisotropic displacement parameters (Å$^2$) for $(NH_4)_2NaMF_6$ ($M$ = Ga, Fe) and $[(NH_4)_{0.83}K_{0.17}]_2KAlF_6$

| Compounds | Atoms | $U_{11}$ | $U_{22}$ | $U_{33}$ |
|---|---|---|---|---|
| $(NH_4)_2NaGaF_6$ | Ga1 | 0.0147(6) | 0.0147(6) | 0.0147(6) |
| | Na1 | 0.0208(14) | 0.0208(14) | 0.0208(14) |
| | F1 | 0.0310(13) | 0.0310(13) | 0.0146(19) |
| | N1 | 0.021(2) | 0.021(2) | 0.021(2) |
| $(NH_4)_2NaFeF_6$ | Fe1 | 0.0154(6) | 0.0154(6) | 0.0154(6) |
| | Na1 | 0.0202(12) | 0.0202(12) | 0.0202(12) |
| | F1 | 0.0352(13) | 0.0352(13) | 0.0163(16) |
| | N1 | 0.0217(18) | 0.0217(18) | 0.0217(18) |
| $[(NH_4)_{0.83}K_{0.17}]_2KAlF_6$ | Al1 | 0.0160(6) | 0.0160(6) | 0.0160(6) |
| | K1 | 0.0188(6) | 0.0188(6) | 0.0188(6) |
| | F1 | 0.0897(14) | 0.0897(14) | 0.0142(12) |
| | N1 (K2) | 0.0286(19) | 0.0286(19) | 0.0286(19) |

12-coordinated site $A$ and the 6-coordinated site $B$ are well suited for the large ammonium ion and the smaller sodium ion, respectively, hence an order mode in the $(NH_4)_2NaMF_6$ structure ($A_2BMF_6$). Also, the ionic radius ratio ($B/A$) may be the main factor for the apparent H-bonding that induced disorder at the F site in the **(AI)** compound. The roomier lattice of the **(AI)** phase relative to its Na analogues offers more chance for displacement of the small F atoms. Similar features have been observed previously in the compounds of $(NH_4)_3FeF_6$ and $(NH_4)_3AlF_6$ [18].

The structure of $(NH_4)_2NaFeF_6$ has been well refined, except that the $R_w$ value of 0.0749 is three times larger than the $R$ value of 0.0216 (Table 1). Similar results also occur in the structures of the gallium analogue and the previously reported compound of $(NH_4)_3FeF_6$ in Ref. [18]. In the difference electron-density map, the highest residual peak (0.34 e/Å$^3$) to its nearest atom Fe is 0.96 Å, and the deepest residual hole (−0.66 e/Å$^3$) is correctly located at the position of the Fe atom. The value of the highest residual peak is small enough for the final refinement, but significantly larger than that of the second highest peak (0.18 e/Å$^3$). In addition, the value of the highest peak is only half of the absolute value of the deepest hole. All of these data indicated that Fe atoms may be distributed in a partially disorder mode. Refinement of the Fe atoms in a disorder mode led to $R = 0.0163$ and $R_w = 0.0415$, as well as max diff. density 0.218 e/Å$^3$ and min −0.230 e/Å$^3$, suggesting that the disordered model is more reliable. However, the refinement showed only 3.7(8)% Fe atoms likely distributed in a disorder mode, and abnormal ratio of $R_w$ vs $R$ could be caused by various other factors. Therefore, Fe disorder, if present, is negligibly small. In combination with results from previous studies [14,15], we suggest that atoms in all elpasolite-type sodium ammonium hexafluorometallates(III) known hitherto show limited disorder at room temperature.

The observed partial substitution between potassium and ammonium in the compound **(AI)** led us to attempt structural refinements allowing substitution between sodium and ammonium. However, the refined site occupancies of Na and N, as free

**Table 4**
Selected bond distances, angles and ionic radii for $(NH_4)_2NaMF_6$($M$ = Ga, Fe, Cr) and $[(NH_4)_{0.83}K_{0.17}]_2KAlF_6$

| $(NH_4)_2NaGaF_6$ | $(NH_4)_2NaFeF_6$ | $[(NH_4)_{0.83}K_{0.17}]_2KAlF_6$ | $(NH_4)_2NaCrF_6$ |
|---|---|---|---|
| Ga1–F1 1.894(4) ( × 6) | Fe1–F1 1.929(3) ( × 6) | Al1–F1 1.789(2) ( × 6) | Cr1–F1 1.9214(11) ( × 6) |
| Na1–F1 2.331(4) ( × 6) | Na1–F1 2.312(3) ( × 6) | K1–F1 2.573(2) ( × 6) | Na1–F1 2.3022(11) ( × 6) |
| $(NH_4)$–F1 2.996(3) ( × 12) | $(NH_4)$–F1 3.005(3) ( × 12) | $(NH_4)$–F1 3.109(11) ( × 12) | $(NH_4)$–F1 2.9926(11) ( × 12) |
| F1–H1 2.29 | F1–H1 2.31 | F1–H1 2.36 | F1–H1 2.30 |
| N1–H1 0.87 | N1–H1 0.87 | N1–H1 0.89 | N1–H1 0.86 |
| F1–H1–N1 137.6 | F1–H1–N1 137.0 | F1–H1–N1 141.8 | F1–H1–N1 137.6 |
| $R_{(NH_4)} = 1.717$ | $R_{(NH_4)} = 1.719$ | – | $R_{(NH_4)} = 1.715$ |
| $R'_{(NH_4)} = 1.740$ | $R'_{(NH_4)} = 1.736$ | – | $R'_{(NH_4)} = 1.743$ |

$R_{(NH_4)}$ denotes a radius of the ammonium ion, which was calculated from the equation of $(r_A+r_F)/d_{A-F} = -0.09472\,(r_B+r_M)+1.1724$ (where $d_{A-F}$ is the bond distance of $A$–F; $r_A$, $r_B$, $r_M$ and $r_F$ are the ionic radii of the corresponding ions in the general formula $A^I_2B^IM^{III}F_6$). This equation was derived from the elpasolite structures known up to now using Shannon's radii (Cs: 1.88 Å, Rb: 1.72 Å and K: 1.64 Å for CN = 12; Rb: 1.52 Å, K: 1.38 Å, Na: 1.02 Å, Li: 0.76 Å and F: 1.33 Å for CN = 6). $R'_{(NH4)}$ means a radius of the ammonium ion, which was calculated from Wassa and Babel's equation of $a_c = 1.289r_A+1.104r_B+1.518r_M+3.222r_F$ (where $r_F = 1.285$ Å (for CN = 2) instead of 1.33 Å).

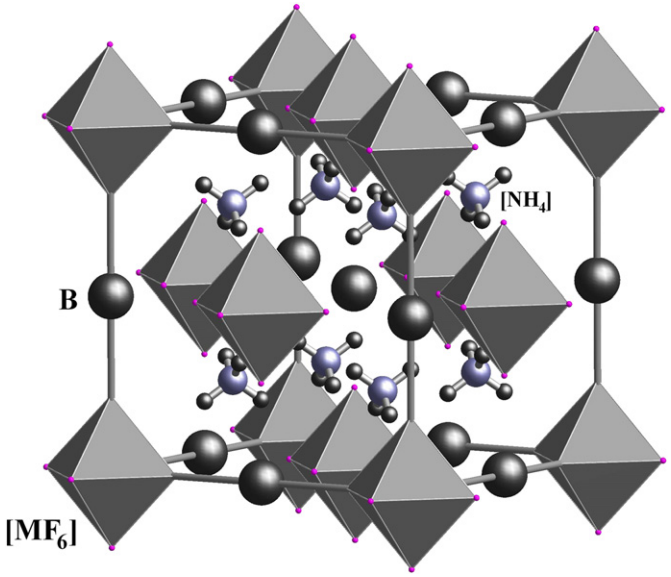


**Fig. 5.** The crystal structure of $(NH_4)_2NaMF_6$ ($M$ = Ga, Fe, Cr) and $[(NH_4)_{0.83}K_{0.17}]_2KAlF_6$.

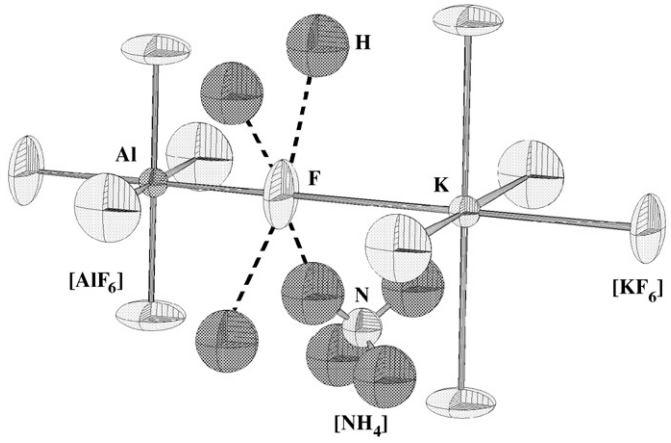


**Fig. 6.** The coordination environments of the metal atoms in $[(NH_4)_{0.83}K_{0.17}]_2KAlF_6$, with displacement ellipsoids drawn at the 50% probability level.

variables, are 0.98(3) and 1.06(4), respectively, close to stoichiometric values for the compound (**Fe**). Admittedly, the X-ray scattering powers of $NH_4^+$ and $Na^+$ are similar, preventing any precise determination whether solid solution between them exists or not. The calculated bond valences of sodium at 1.08, 1.02 and 1.11 for compounds **(Fe)**, **(Ga)** and **(Cr)**, respectively [21], indicate that sodium has a normal bond length in all three cases. On the basis of chemical analyses reported in previous studies [13–15], substitution between sodium and ammonium in sodium ammonium hexafluorometallates(III) is most likely very limited. The size difference may be the reason why $[(NH_4)_{2-x}K_x]KAlF_6(x = 0,1)$ is the only available example that displays a solid solution between $NH_4^+$ and $K^+$ in the A site. Further investigation is needed to determine whether substitution between ammonium and potassium (and between ammonium and rubidium) occurs in the (Fe, Ga, Cr, V) analogues of $[(NH_4)_{2-x}K_x]KAlF_6$ [13].

Massa and Babel [1] proposed the following equation for calculating cell parameters for the elpasolite-type compounds:

$$a_c = 1.289r_A + 1.104r_B + 1.518r_M + 3.222r_F \quad (1)$$

They claimed that agreement between the observed and calculated lattice constants was better than 0.5% in the worst cases and 0.1% on the average. They also suggested that Eq. (1) might also be used to calculate ionic radii, especially those for the unusual $M^{III}$ oxidation states stabilized in cubic elpasolites. It is noteworthy that the comprehensive compilation of ionic radii by Shannon [22] did not include the ammonium ion. In general, the radius of the ammonium ion for CN = 8 is believed to be the same with that of rubidium ion ($Rb^+$ = 1.48 Å) [23]. There have been no data for the ionic radius of the ammonium ion for CN = 12. The radii of the ammonium ion (CN = 12) in compounds (**Ga**), (**Fe**) and (**Cr**) have been calculated by use of Eq. (1), including a mean value of 1.740 Å (Table 4).

On the basis of 63 known structures (Fig. 7), we propose an alternative equation:

$$(r_A + r_F)/d_{A-F} = -0.09472(r_B + r_M) + 1.1724 \quad (2)$$

where $d_{A-F}$ is the bond distance of $A$–F; and $r_A$, $r_B$, $r_M$ and $r_F$ are the ionic radii of the corresponding ions in the formula $A^I_2B^IM^{III}F_6$. The equation in Fig. 7 has a correlation coefficient $R = -0.85$ and probability $P < 0.0001$(that $R$ is zero). Fig. 7 shows that Eq. (2) fits the experimental data well by excluding a few large-offset cases (e.g. lithium analogues). The mean value of the ammonium ionic radius from Eq. (2) is 1.717 Å, which is somewhat smaller than that from Eq (1). It is generally believed that the ionic radius of ammonium is larger than that of potassium but similar to that of rubidium. We herein adopt an average value of 1.729 Å from Eqs. (1) and (2).

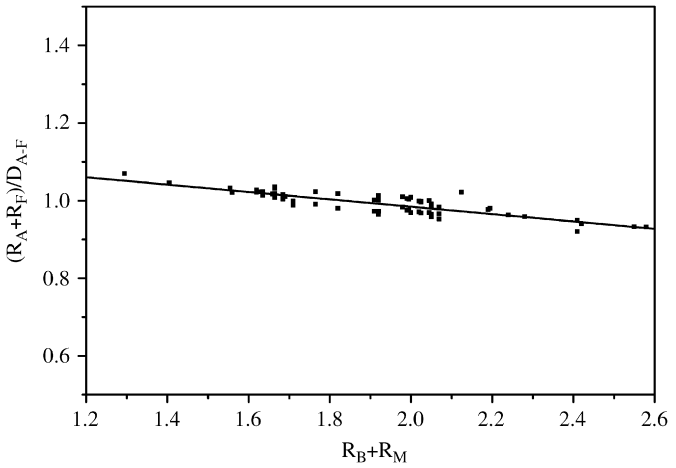


**Fig. 7.** Linear dependence between the $(R_A+R_F)/D_{A-F}$ and the $R_B+R_M$ (where $d_{A-F}$ is the bond distance of *A*–F; $r_A$, $r_B$, $r_M$ and $r_F$ are the ionic radii of the corresponding ions in the general formula $A^{I}_{2}B^{I}M^{III}F_6$).

### 3.2. Spectroscopy analysis

The internal modes of the free $NH_4^+$ group having the $T_d$ symmetry are expected at 3040($\nu_1$), 1680($\nu_2$), 3145($\nu_3$) and 1400($\nu_4$) $cm^{-1}$. Factor-group analysis of $NH_4^+$ with the $T_d$ symmetry predicts $\nu_1(A_1)$ and $\nu_2(E)$ active only for Raman, and $\nu_3(F_2)$ and $\nu_4(F_2)$ active for both Raman and IR [24]. In the compound **(Cr)** ammonium ions are located at the symmetry site of $\bar{4}3m$ (at 8*c*) and have a $T_d$ symmetry, same as a free $NH_4^+$ group. Fig. 1 shows that the FTIR spectrum of the compound (**Cr**) consists of three main absorption peaks. The two at 3269 and 1428 $cm^{-1}$ can be unambiguously attributed to the asymmetric stretching $\nu_3$ and bending $\nu_4$ vibrations of ammonium ions, respectively, whereas the other one at 520 $cm^{-1}$ is assigned to the [$CrF_6$] group. Although the frequency (3269 $cm^{-1}$) of $\nu_3(F_2)$ observed in this study is significantly larger than that ($\nu_3 = 3145\ cm^{-1}$) for a free $NH_4^+$ group, it is consistent with the result ($\nu_3 = 3275\ cm^{-1}$) reported in Ref. [25]. Other weak absorption peaks can be divided into two sets. One set of bands at 3095, 2927, 2858, and 1642 $cm^{-1}$ have larger frequencies than 1428 $cm^{-1}$, are caused by overlapping, overtone and combination of the $\nu_3$ and $\nu_4$ vibrations of ammonium ions. The other set of bands at 1081 and 741 $cm^{-1}$ have smaller frequencies than 1428 $cm^{-1}$, are tentatively attributed to the [$CrF_6$] group. The Raman spectrum of the compound **(Cr)** is composed of a strong peak at 3195 $cm^{-1}$, which is assigned to the asymmetric stretching $\nu_3$ vibration of ammonium ions, two intermediate peaks at 544 and 263 $cm^{-1}$ ascribed to the [$CrF_6$] group, and four weak peaks (Fig. 2). Three of the weak peaks at 1438, 1699 and 2845 $cm^{-1}$ are assigned to the asymmetric bending $\nu_4$, symmetric bending $\nu_2$, and overtone of $\nu_4$ vibrations, respectively; the forth one at 200 $cm^{-1}$ may be caused by lattice vibration. The aluminum analogue of the compound (**Cr**) was prepared as described in Ref. [12], and its FTIR and Raman spectra and peak assignments are given in Table 5 for comparison.

Investigation of luminescence and optical absorption on materials doped with octahedrally coordinated $Cr^{3+}$ is another intensive research topic in the elpasolite system. In an octahedral $d^3$ metal complex, $CrF_6^{3-}$, it has the following spin-allowed transitions: $^4A_{2g} \rightarrow {}^4T_{2g}$(F) and designated as $E_1$, $^4A_{2g} \rightarrow {}^4T_{1g}$ (F) and designated as $E_2$, and $^4A_{2g} \rightarrow {}^4T_{1g}$ (P) and designated as $E_3$. The energy value of $E_1$ is equivalent to 10Dq, and that of $E_2$ and $E_3$ is given respectively as

$$E_2 = 15\mathrm{Dq} + 7.5\mathrm{B} - 6\mathrm{B}(1+\mu)^{1/2} \quad (3)$$

$$E_3 = 15\mathrm{Dq} + 7.5\mathrm{B} + 6\mathrm{B}(1+\mu)^{1/2} \quad (4)$$

**Table 5**
IR and Raman wavenumbers ($cm^{-1}$) for $(NH_4)_2NaCrF_6$ and $(NH_4)_2NaAlF_6$

| $(NH_4)_2NaCrF_6$ | | | | $(NH_4)_2NaAlF_6$ | | | |
|---|---|---|---|---|---|---|---|
| IR | Assign. | Raman | Assign. | IR | Assign. | Raman | Assign. |
| 3269 vs | $\nu_3$ ($F_2$) | 3195 vs | $\nu_3$ ($F_2$) | 3284 vs | $\nu_3$ ($F_2$) | 1649 vs | $\nu_2$(E) |
| 3095 sh | | 2845 vw | $2\nu_4$ ($F_2$) | 3105 w | | 1613 m | |
| 2927 vw | | 1699 w,br | $\nu_2$(E) | 2922 vw | | 1445 vw | $\nu_4$ ($F_2$) |
| 2858 vw | $2\nu_4$ ($F_2$) | 1438 vw | $\nu_4$ ($F_2$) | 2848 vw | $2\nu_4$ ($F_2$) | 544 w | [$CrF_6$] |
| 1642 vw | | 544 m | [$CrF_6$] | 1431 vs | $\nu_4$ ($F_2$) | 319 vw | [$CrF_6$] |
| 1428 vs | $\nu_4$ ($F_2$) | 263 m | [$CrF_6$] | 727 m | [$AlF_6$] | 213 w | |
| 1081 w | [$CrF_6$] | 200 w | | 563 vs | [$AlF_6$] | | |
| 741 w | [$CrF_6$] | | | 451 w | [$AlF_6$] | | |
| 520 vs | [$CrF_6$] | | | | | | |

Relative intensities: v, very; s, strong; m, medium; w, weak; sh, shoulder; br, broad.

where $\mu = [(10\,\mathrm{Dq} - 9B)/12B]^2$. Eqs. (3) and (4) were derived from Tanabe and Sugano's (1954) matrix [26]; the *B* value is then determined from the energies of the $E_1$ and $E_2$ transitions by means of the relationship [27]:

$$B = [(2E_1 - E_2)(E_2 - E_1)]/[3(9E_1 - 5E_2)] \quad (5)$$

The *B* value also can be calculated from the energies of the $E_2$ and $E_3$ by the following equation:

$$B = (E_2 + E_3)/15 - 2\mathrm{Dq} \quad (6)$$

The absorption spectrum of $(NH_4)_2NaCrF_6$ as shown in Fig. 3, contains a broad triplet band and two main single bands. The broad triplet band is overlapped by some structures, and consists of 635 nm (15 748 $cm^{-1}$), 654 nm (15 290 $cm^{-1}$) and 610 nm (16 393 $cm^{-1}$). This triplet band is tentatively interpreted to be caused by the spin-allowed transition from the ground state $^4A_{2g}(^4F)$ of the $Cr^{3+}$ ion to the orbital $^4T_{2g}(^4F)$ ($E_1 = 15\,748\ cm^{-1}$) and the spin-forbidden transitions from the ground state $^4A_{2g}(^4F)$ to the $^2E_g(^2G)$ ($E_4 = 15\,290\ cm^{-1}$) and $^2T_{1g}(^2G)$ ($E_5 = 16\,393\ cm^{-1}$) orbitals. The other two main bands centered at 436 and 285 nm (or $E_2 = 22\,936\ cm^{-1}$ and $E_3 = 35\,088\ cm^{-1}$) can be unambiguously ascribed to the orbitals $^4T_{1g}(^4F)$ and $^4T_{1g}(^4P)$, respectively. These observed values ($E_1 = 15\,748\ cm^{-1}$, $E_2 = 22\,936\ cm^{-1}$, and $E_3 = 35\,088\ cm^{-1}$) give two different solutions by use of Eqs. (5) and (6). We prefer the value calculated from Eq. (5), because it gives the best fit on the Tanabe–Sugano diagram plotted by the program of Ref. [28]. Our preference is also consistent with the suggestion in Ref. [27] that $E_3$ is not suitable for the calculation of the *B* parameter. Therefore, the crystal field strength Dq, and Racah parameters *B* and Dq/*B* of the compound (**Cr**) have the following values (in $cm^{-1}$): 1575, 758, 2.1. According to Ref. [29], for $1.5 < \mathrm{Dq}/B < 3.5$ the Racah parameter C can be obtained from Eq. (7) with 0.5% of relative accuracy as compared to the value obtained by matrices diagonalization [7]:

$$E_4(^4A_2 - {}^2E)/B = 3.05C/B + 7.09 - 1.8B/\mathrm{Dq} \quad (7)$$

We can also use the expression (8) of the $^2T_1$ level to calculate the Racah parameter *C* [30]:

$$E_5(^4A_2 - {}^2T_1) = 9B + 3C - 24B/10\mathrm{Dq} \quad (8)$$

A mean value of $C = 3374\ cm^{-1}$ has been obtained by use of Eqs. (7) and (8), and *C*/*B* of 4.45. These values are close to those obtained for octahedrally coordinated $Cr^{3+}$ in other elpasolites [6,7]. The degree of covalency of a metal–ligand bond in a complex may

**Table 6**
A comparison of observed and calculated data of the ultraviolet– visible absorption spectrum$(NH_4)_2NaCrF_6$ at room temperature

| Assignment | Observed | Calculated |
|---|---|---|
| $^4A_{2g}\rightarrow{}^2E_g(^2G)$ | 15290 | 15656 |
| $^4A_{2g}\rightarrow{}^4T_{2g}(^4F)$ | 15748 | 15748 |
| $^4A_{2g}\rightarrow{}^2T_{1g}(^2G)$ | 16393 | 16353 |
| $^4A_{2g}\rightarrow{}^4T_{1g}(^4F)$ | 22936 | 22934 |
| $^4A_{2g}\rightarrow{}^2T_{2g}(^2G)$ | | 23253 |
| $^4A_{2g}\rightarrow{}^2A_{1g}(^2G)$ | | 29012 |
| $^4A_{2g}\rightarrow{}^2T_{2g}(^2H)$ | | 31278 |
| $^4A_{2g}\rightarrow{}^2E_g(^2H)$ | | 33680 |
| $^4A_{2g}\rightarrow{}^4T_{1g}(^4P)$ | 35088 | 35678 |
| $^4A_{2g}\rightarrow{}^2T_{1g}(^2H)$ | | 36938 |
| $^4A_{2g}\rightarrow{}^2T_{2g}(^2D)$ | | 42663 |

be determined using the covalency parameter, $\beta$, which is equivalent to the ratio of the Racah parameter $B$ in the complex to that of the free cation, $B_o$ in Refs. [26,31]. $B = 758\,cm^{-1}$ obtained in this study for the compound **(Cr)** divided by the free-ion value ($B_o = 918\,cm^{-1}$, in Ref. [32]) gives a $\beta$ factor of 0.83, reflecting the covalency effect. With the above assumption and combined spin–orbit interaction and crystal field matrices, we calculated the energy level scheme of the $(NH_4)_2NaCrF_6$ by use of the program of Ref. [28]. The calculated and observed values are in excellent agreement (Table 6).

### 3.3. Crystal growth

It is well known that impurities can have a large effect on crystal morphology. For example, the Donnay–Harker law [33] predicts the frequency of crystal forms for NaCl ($Fm\bar{3}m$) in order of {111}, {200}, {021}, {112}… However, natural NaCl usually occurs in cubes, which has been attributed to the addition of small quantities of impurities [34,35]. The similarity in space group between the elpasolite-type compounds and NaCl intrigued our investigation on crystal morphology. In this study, only polycrystalline powder was obtained for the compound **(Cr)**. We were unable to synthesize large crystals of **(Cr)** for a single-crystal X-ray diffraction study. In contrast, suitable single crystals were grown easily for compounds (**Fe)** and (**Ga**), but we could not obtain pure samples for them. As described in above, sporadic octahedral shaped crystals of (**Fe)** and **(Ga)** are wrapped in polycrystalline powder $Fe(NH_4)HP_3O_{10}$ and $Ga(NH_4)HP_3O_{10}$, respectively. We suggest that there is a linkage between the octahedral crystals and the matrix materials on their surface. Figs. 8 and 9 show the crystal structure of the compound **(Fe)** projected to the plane (111) [36,37] and that of $Fe(NH_4)HP_3O_{10}$ [38] to $(10\bar{1})$, respectively. The interval between two $[FeF_6]$ octahedra labeled by sites *A* and *B* in the compound (**Fe)** is 10.39 Å (Fig. 8), which is almost the same as the distance (10.41 Å) between $[FeO_6]$ octahedra marked by *A* and *B* in $Fe(NH_4)HP_3O_{10}$. Therefore, the direction from octahedron *A* to octahedron *B* is $[10\bar{1}]$ in the compound (**Fe)**, and $[1\bar{2}1]$ in $Fe(NH_4)HP_3O_{10}$. Furthermore the distance between octahedra of site *B* and *C* with direction $[11\bar{2}]$ in the compound (**Fe)** is about 6.00 Å, also approximately similar to that (6.08 Å) with direction [101] in $Fe(NH_4)HP_3O_{10}$. Therefore, the {111} face of the compound **(Fe)** is stabilized by a two-dimensional epitaxial adsorption layer of $Fe(NH_4)HP_3O_{10}$ $(10\bar{1})$. The $(NH_4)_2NaFeF_6$ (111) and $Fe(NH_4)HP_3O_{10}(10\bar{1})$ faces have a misfit of +1.4%. A similar case occurs also for the pair between $(NH_4)_2NaGaF_6$ (111) and $Ga(NH_4)HP_3O_{10}(10\bar{1})$. Therefore, the occurrences of faceted octahedra of the compounds (**Fe**) and (**Ga**) are most linked to the phosphate impurities.

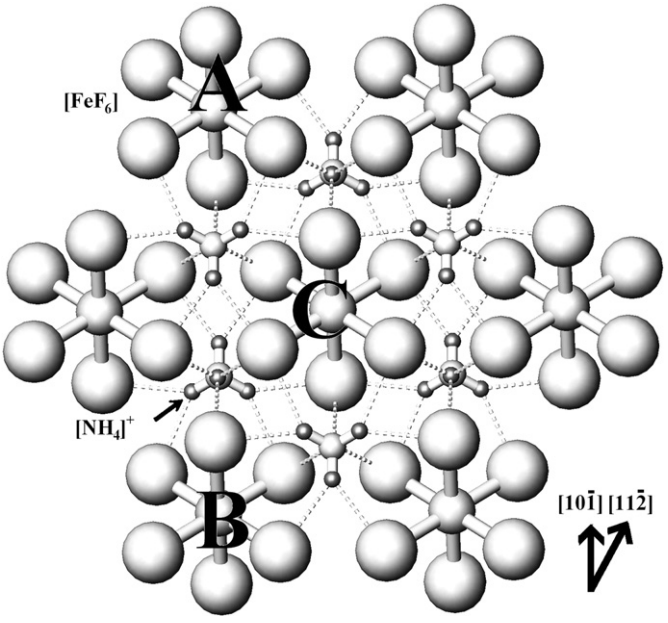


**Fig. 8.** Projection of the crystal structure of $(NH_4)_2NaFeF_6$ to the plane (111).

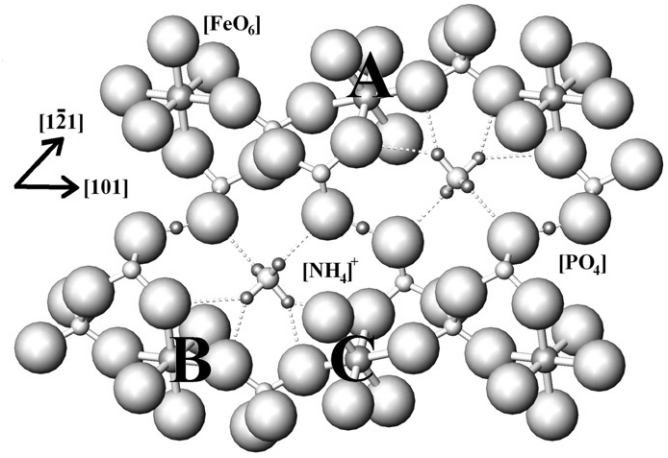


**Fig. 9.** Projection of the crystal structure of $Fe(NH_4)HP_3O_{10}$ to the plane $(10\bar{1})$.

## 4. Conclusions

Our X-ray structural analyses and previous studies show that all atoms in all elpasolite-type ammonium sodium hexafluorometallates(III), $(NH_4)_2NaMF_6(M = Al, Cr, Fe, Ga, In)$, are largely in order modes. A crystal field ($Dq = 1575\,cm^{-1}$) and Racah parameters ($B = 758\,cm^{-1}$, $C = 3374\,cm^{-1}$, $Dq/B = 2.08$, and $C/B = 4.45$) for $(NH_4)_2NaCrF_6$ have been determined from a room-temperature optical absorption spectrum. The phase transition of the compound $(NH_4)_2KAlF_6$ at low temperature has a close relationship with the abnormal anisotropic thermal parameters of the fluorine atoms, which are caused by four strong hydrogen bonds (F…H–N) distributed in a square form around each fluorine atom.

## Acknowledgments

The authors are indebted to the National Natural Science Foundation of China (No. 40472027) for financial support. We are

also grateful to three referees for their comments and suggestions on the original draft of the manuscript.

## References

[1] W. Massa, D. Babel, Chem. Rev. 88 (1988) 275–296.
[2] I.N. Flerov, M.V. Gorev, K.S. Aleksandrov, A. Tressaud, J. Grannec, M. Couzi, Mater. Sci. Eng. R 24 (3) (1998) 81–151.
[3] Y. Xu, S. Carlson, A. Sjödin, R. Norrestam, J. Solid State Chem. 150 (2000) 399–403.
[4] Y. Xu, K. Söderberg, R. Norrestam, J. Solid State Chem. 153 (2000) 248–253.
[5] M.V. Gorev, I.N. Flerov, A. Tressaud, A.I. Zaitsev, E. Durand, Solid State Sci. 4 (2002) 15–18.
[6] L.P. Sosman, A.D. Tavares Jr., R.J.M. da Fonseca, T. Abritta, N.M. Khaidukov, Solid State Commun. 114 (2000) 661–665.
[7] M.A.F.M. da Silva, R.B. Barthem, L.P. Sosman, J. Solid State Chem. 179 (2006) 3718–3723.
[8] J.A. Aramburu, M. Moreno, K. Doclo, C. Daul, M.T. Barriuso, J. Chem. Phys. 110 (1999) 1497–1507.
[9] M.G. Brik, C.N. Avram, N.M. Avram, Physica B 384 (2006) 78–81.
[10] K. Moriya, T. Matsuo, H. Suga, S. Seki, Bull. Chem. Soc. Japan 50 (1977) 1920–1926.
[11] K. Moriya, T. Matsuo, H. Suga, S. Seki, Bull. Chem. Soc. Japan 52 (1979) 3152–3162.
[12] A. Tressaud, S. Khaïroun, L. Rabardel, T. Kobayashi, T. Matsuo, H. Suga, Phys. Stat. Sol. A 96 (1986) 407–414.
[13] W. Massa, Z. Anorg. Allg. Chem. 427 (1976) 235–240.
[14] A. Roloff, D. Trinschek, M. Jansen, Z. Anorg. Allg. Chem. 621 (1995) 737–739.
[15] S.-M. Luo, C.-X. Wang, X.-X. Liu, Z.-B. Wei, J.-X. Mi, Acta Cryst. E 62 (2006) i179–i181.
[16] I.N. Flerov, M.V. Gorev, J. Grannec, A. Tressaud, J. Fluorine Chem. 116 (2002) 9–14.
[17] K. Hirokawa, Y. Furukawa, J. Phys. Chem. Solids 49 (1988) 1047–1056.
[18] A.A. Udovenko, N.M. Laptash, I.G. Maslennikova, J. Fluorine Chem. 124 (2003) 5–15.
[19] G.M. Sheldrick, SHELXS-97, Program for the solution of crystal structures; University of Göttingen, Göttingen, 1997. SHELXL-97, Program for the refinement of crystal structures, University of Göttingen, Göttingen, 1997.
[20] (a) A.C. Larson, R.B. Von Dreele, GSAS. Los Alamos National Laboratory, New Mexico, USA, 2000;
(b) B.H. Toby, J. Appl. Cryst. 34 (2001) 210–213.
[21] N.E. Brese, M. O'Keeffe, Acta Crystallogr. B 47 (1991) 192–197.
[22] R.D. Shannon, Acta Crystallogr. A 32 (1976) 751–767.
[23] F.A. Cotton, G. Wilkinson, Advanced Inorganic Chemistry, fifth ed., Wiley, New York, 1988, p. 315.
[24] K. Nakamoto, Infrared and Raman Spectra of Inorganics and Coordination Compounds (Part A & B), fifth ed., Wiley, New York, 1997.
[25] E. Srasra, F. Bergaya, J.J. Fripiat, Clays Clay Miner. 42 (1994) 237–241.
[26] Y. Tanabe, S. Sugano, J. Phys. Soc. Japan 9 (1954) 753–799.
[27] R.M. Abu-Eid, R.G. Burns, Am. Mineral. 61 (1976) 391–397.
[28] R.J. Lancashire, JAVA applet for Tanabe-Sugano diagrams, University of the West Indies, Jamaica, 2006.
[29] B. Henderson, G.F. Imbusch, Optical Spectroscopy of Inorganic Solids, Clarendon Press, Oxford, 1989.
[30] M. Mortier, Q. Wang, J.Y. Buzare, M. Rousseau, Phys. Rev. B 56 (1997) 3022–3031.
[31] C.K. Jorgensen, Prog. Inorg. Chem. 4 (1962) 73.
[32] J.S. Griffith, The Theory of Transition Metal Ions, Cambridge University Press, London, 1964.
[33] J.D.H. Donnay, D. Harker, Am. Mineral. 22 (1937) 446–467.
[34] N. Radenović, D. Kaminski, W. Enckevort, S. Graswinckel, I. Shah, M. Veld, R. Algra, E. Vliega, J. Chem. Phys. 124 (2006), 164706-6.
[35] N. Radenović, W. Enckevort, P. Verwer, E. Vlieg, Surf. Sci. 523 (2003) 307–315.
[36] Shape Software, Atoms V6.1, 521 Hidden Valley Road, Kingsport, TN 37663, USA, 2004.
[37] K. Brandenburg, Diamond Version 3.0, Crystal Impact GbR, Bonn, Germany, 1997–2004.
[38] V.V. Krasnikov, Z.A. Konstant, V.S. Fundamenskii, Neorganicheskie Mater. 19 (1983) 1373–1378.